

Astrometry with the MCAO instrument MAD

An analysis of single-epoch data obtained in the layer-oriented mode[★]

E. Meyer^{1,2}, M. Kürster¹, C. Arcidiacono^{3,4}, R. Ragazzoni³, and H.-W. Rix¹

¹ Max Planck Institute for Astronomy (MPIA), Königstuhl 17, 69117 Heidelberg, Germany

² Leiden Observatory, Leiden University, P.O. Box 9513, 2300 RA Leiden, The Netherlands
e-mail: meyer@strw.leidenuniv.nl

³ INAF Osservatorio Astronomico di Padova, Vicolo dell'Osservatorio, 5, 35122 Padova, Italy

⁴ INAF Osservatorio Astrofisico di Arcetri, Largo Enrico Fermi, 5, 50125, Firenze, Italy

Received November 3, 2010; accepted May 11, 2011

ABSTRACT

Context. Current instrument developments at the largest telescopes worldwide have provisions for Multi-Conjugated Adaptive Optics (MCAO) modules. The large field of view and more uniform correction provided by these systems is not only highly beneficial for photometric studies but also for astrometric analysis of, e.g., large dense clusters and exoplanet detection and characterization. The Multi-conjugated Adaptive optics Demonstrator (MAD) is the first such instrument and was temporarily installed and tested at the ESO/VLT in 2007. We analyzed two globular cluster data sets in terms of achievable astrometric precision. Data were obtained in the layer-oriented correction mode, one in full MCAO correction mode with two layers corrected (NGC 6388) and the other applying ground-layer correction only (47 Tuc).

Aims. We aim at analyzing the first available MCAO imaging data in the layer-oriented mode obtained with the MAD instrument in terms of astrometric precision and stability.

Methods. We calculated Strehl maps for each frame in both data sets. Distortion corrections were performed and the astrometric precision was analyzed by calculating mean stellar positions over all frames and by investigation of the positional residuals present in each frame after transformation to a master-coordinate-frame.

Results. The mean positional precision for stars between $K = 14 - 18$ mag is ≈ 1.2 mas in the full MCAO correction mode data of the cluster NGC 6388. The precision measured in the GLAO data (47 Tuc) reaches ≈ 1.0 mas for stars corresponding to 2MASS K magnitudes between 9 and 12. The observations were such that stars in these magnitude ranges correspond to the same detector flux range. The jitter movement used to scan a larger field of view introduced additional distortions in the frames, leading to a degradation of the achievable precision.

Key words. technique: image processing – instrumentation: adaptive optics, MCAO – methods: astrometry – globular cluster: individual: NGC 6388, 47 Tuc

1. Introduction

In classical adaptive optics correction, with one reference star, the field of view (FoV) is limited by the effect of anisoplanatism, as only the integrated phase error over the column above the telescope in the direction to the guide star is measured and corrected. Turbulence outside this column, e.g. in the direction of the target, if it cannot be used itself as guide star, is not mapped and the correction degrades rapidly with growing separation to the guide star. The average wavefront phase error is limited to < 1 rad only within the so-called isoplanatic angle, which is for typical astronomical sites $10'' - 20''$ in the K -band and only $3''$ in the visible. In the case of a laser guide star as reference source, the phase error is even larger, due to the low focussing altitude and the resulting cone-effect (Tallon & Foy 1990; Yan et al. 2005). Multi Conjugated Adaptive Optics (MCAO;

Beckers 1988; Ellerbroek et al. 1994) is an approach to achieve diffraction limited image quality over larger FoVs of up to 2-4 arcminutes and hence overcome anisoplanatism. Moderate averaged Strehl-ratios, in the range of 10% to 25%, can be achieved, but with a higher uniformity of the Point-Spread-Function (PSF) over the FoV. This is desired for resolving structures of extended sources, such as galaxies or cores of star clusters. In MCAO the 3-dimensional structure of the turbulence is reconstructed by means of the information coming from several guide stars, natural or laser. Instead of correcting the turbulence integrated over a single direction, turbulence from different layers is corrected with several deformable mirrors conjugated to these layers. The maximum achievable performance on the single reference stars is not as good as with classical adaptive optics (AO), due to the turbulence above and below the single corrected layers, but instead the correction is more uniform over a significantly larger FoV. Typically two layers are being corrected, the ground layer close to the telescope and a higher layer at around 8 - 10 km height (dependent on the site). Most of the turbulence in the atmosphere is generated in the ground layer. Correcting only this layer (GLAO=Ground-Layer Adaptive Optics), one can remove the major contributor to the

[★] Based on observations collected at the European Southern Observatory, Paranal, Chile, as part of the MAD Guaranteed Time Observations

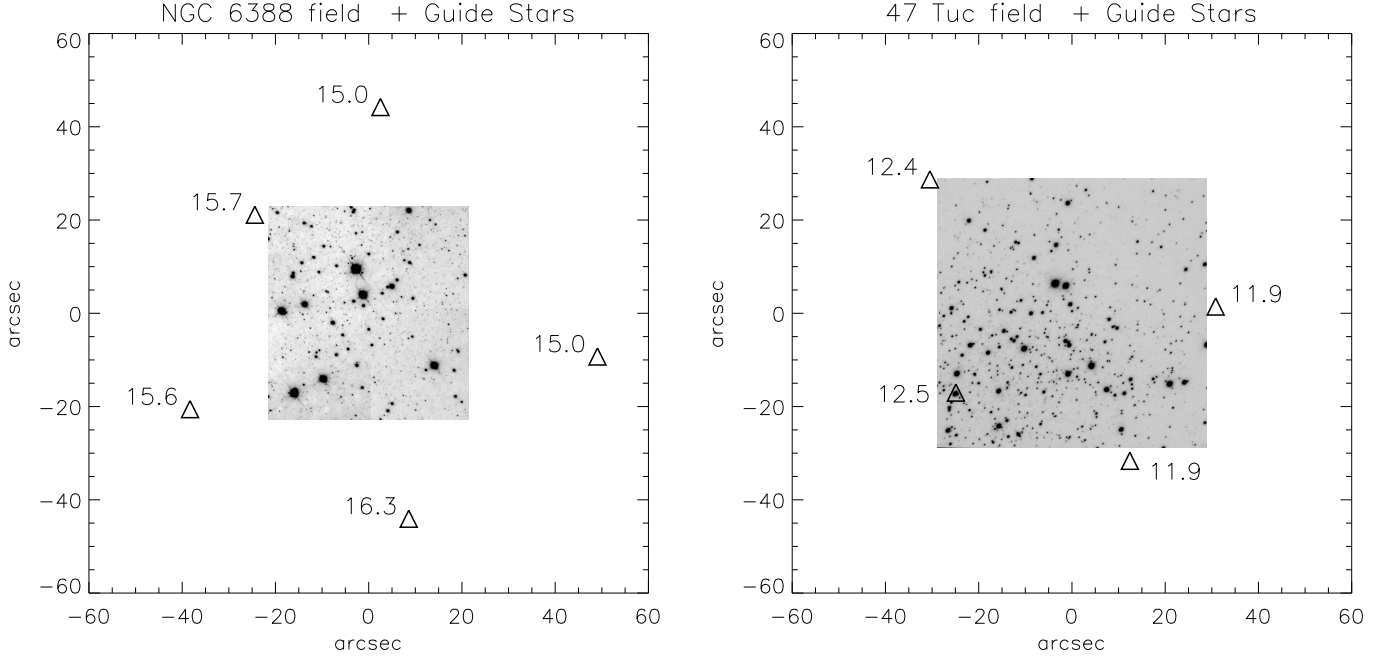


Fig. 1. MAD images of the globular clusters NGC 6388 (left) and 47 Tuc (right). The triangles mark the positions of the AO guide stars relative to center of the observed FoV. The numbers close to the stars correspond to their HST F606W (visual) magnitude.

phase aberrations of the incoming wavefronts (Rigaut 2002). Two different approaches are in use to combine the signals from the different reference stars, the Star Oriented (SO) and the Layer Oriented (LO). In the SO mode, each reference star is observed by one wavefront sensor (WFS) and one detector. The information from the different directions of the guide stars is combined to generate 3D information of the atmosphere within the mapped FoV. In this approach of turbulence tomography (Tallon & Foy 1990) the influence of a single layer can be computed and corrected with one deformable mirror conjugated to this layer. The first verification of this approach was done in an open loop measurement at the Telescopio Nazionale di Galileo (TNG) (Ragazzoni et al. 2000b). In the layer oriented approach (Ragazzoni et al. 2000a), each WFS and detector is conjugated to one layer in the atmosphere instead to a single star. The light of several guide stars is optically co-added to increase the signal-to-noise ratio (SNR) on the detector, such that also fainter stars can be used as guide stars. This increases the sky coverage, the fraction of regions on the sky that can offer a suitable natural asterism, essentially for this approach. Also the number of needed wavefront sensors and detectors is reduced, reducing the detector read-out-noise and the needed computing power compared to the SO approach.

High precision astrometry combined with high angular resolution is essential to many science cases in astronomy. E.g. observations of stars around the supermassive black hole in the center of our own Milky Way (e.g. Trippe et al. 2008; Schödel et al. 2009) and of the central regions of globular clusters are only possible with space-based facilities or adaptive optics supported observations from the ground. Multi-epoch high precision proper motion studies with the Hubble Space Telescope (HST) made it possible to distinguish cluster members from foreground field stars and to study the internal dynamics and kinematics of several globular clusters and galactic starburst clusters (e.g. King & Anderson 2001; McLaughlin et al. 2006; Rochau et al. 2010). Another field of high precision astrometry

is the detection and characterization of extrasolar planets by measuring the astrometric reflex-motion of the star (e.g. Benedict et al. 2002; Bean et al. 2007, FGC/HST), (Meyer et al. 2010, NACO/VLT, in preparation). This is an important technique, complementary to the radial velocity method, the most efficient detection method so far. A larger FoV enhances the number of usable reference stars for the measurement of the relative astrometric motion and therefore the achievable precision significantly.

The Multi-Conjugated Adaptive Optics Demonstrator (MAD) is a prototype instrument for MCAO correction and observation and was installed at the ESO VLT UT3 at the Paranal Observatory in 2007 (Marchetti et al. 2007). MAD was designed to study and test different MCAO systems, both in the lab and on-sky (Hubin et al. 2002; Marchetti et al. 2003; Arcidiacono et al. 2006). MAD employs adaptive optics sensing and correction in the star-oriented and the layer-oriented mode. Two layers are sensed and corrected in the full MCAO mode. The ground-layer at the telescope’s pupil and a high layer at 8.5 km altitude. Future AO instruments will use the MCAO technique, such as the Gemini MCAO System (GeMS) at the Gemini South Observatory on Cerro Pachon, Chile. The Fizeau-Interferometer LINC-NIRVANA for the Large Binocular Telescope (LBT) on Mt. Graham in Arizona, will be equipped with four layer oriented correction units, two for each telescope, which will correct the ground layer and a high layer (e.g. Farinato et al. 2008). One of the science-cases of LINC-NIRVANA will be the detection and characterization of extrasolar planets.

All the above mentioned aspects and the uniqueness of the very first MCAO data available encouraged us to analyse this data in terms of astrometric precision and stability. The aim of this study is the estimation of the achievable precision and stability in astrometric measurements obtained with MCAO imaging.

2. Observations and data reduction

The observations analyzed here were conducted with the multi pyramid wavefront sensor of the MAD instrument in the LO mode (Ragazzoni 1996; Ragazzoni et al. 2000b; Arcidiacono et al. 2008). This sensor has the advantage that it can use up to 8 guide stars simultaneously which can be relatively faint ($V < 18$) and for which the integrated light reaches $V = 13$. A uniform distribution of these stars is preferable but they can be everywhere in the $2' \times 2'$ FoV. A NIR- science camera is used for the observations, which is also used in the SO mode: CAMCAO = Camera for MCAO. It has a $57'' \times 57''$ field of view but can scan a circular FoV of 2 arcmin diameter. The HgCdTe HAWAII2 IR-detector built by Rockwell has 2048×2048 pixels with a pixel-scale of $0.028''/\text{px}$, a readout-noise of 13.8 erms, a full well capacity of 65000 ADU and a loss of linearity above 35000 ADU. Two data sets were analyzed, one in the globular cluster NGC 6388 and the other one in the globular cluster 47 Tuc. Both data sets are test data obtained during the first on-sky test of the LO correction mode with MAD at the VLT.

The goal of the observations was to verify and show the capabilities of MCAO observations in LO mode. The original focus was the photometric analysis, as especially high precision photometric studies in crowded fields, like clusters, benefit from the large AO-corrected FoV. Therefore note that the observations analyzed here were not obtained under the aspect of high precision astrometry. Nevertheless they represent a unique data set to investigate the possibilities of high precision astrometry with MCAO.

2.1. MCAO - NGC 6388

The data of the globular cluster NGC 6388 were obtained on September 27th 2007 using the full MCAO capability of MAD. The observations were made in the K_s band (central wavelength = $2.12 \mu\text{m}$) using 5 guide stars with $V = 15.0, 15.0, 15.6, 15.7$ and 16.3 mag^1 , corresponding to an integrated magnitude of 13.67 (Arcidiacono et al. 2008). The guide stars are positioned around the field of view, see Fig. 1, left. The observed field lies at the south-eastern rim of the cluster at RA(J2000)=17:36:22.86, DEC(J2000)=-44:45:35.53. Altogether 30 frames were obtained, the first five in GLAO mode and the last 25 in full MCAO mode. A jitter pattern of five positions was used, repeated six times with three slightly different central points, to scan part of the $2' \times 2'$ FoV, avoid bad pixel incidents and for better sky estimation. The first 10 frames were obtained with a Detector Integration Time of DIT = 10 seconds and $N = 24$ of these DITs (=NDIT) are directly co-added onto one frame, resulting in 240 seconds total exposure time per frame. In the last 20 frames the number of exposures was reduced to NDIT = 12, resulting in 120 seconds total integration time per frame. In Table 1 the observations are summarized together with performance indicators such as the FWHM of the fitted PSF and the seeing measured by the DIMM monitor. The same data was also analyzed for photometry by Moretti et al. (2009).

2.2. GLAO - 47 Tuc

The observations of the globular cluster 47 Tuc were obtained on September 22nd 2007 using only the Ground Layer Adaptive Optics approach (Arcidiacono et al. 2008). The center of the

Table 1. Summary of the observations of the clusters NGC 6388 and 47 Tuc.

frame	NGC 6388			47 Tuc		
	ExpT [sec]	seeing V ["]	FWHM K_s ["]	ExpT [sec]	seeing V ["]	FWHM Bry ["]
1	240	0.43	0.098	30	1.09	0.178
2	240	0.41	0.094	30	1.15	0.186
3	240	0.49	0.099	30	1.13	0.206
4	240	0.55	0.094	30	1.08	0.169
5	240	0.51	0.090	30	1.09	0.178
6	240	0.41	0.095	30	1.08	0.147
7	240	0.38	0.097	30	1.15	0.157
8	240	0.37	0.098	30	1.17	0.193
9	240	0.39	0.103	30	1.17	0.173
10	240	0.40	0.106	30	1.15	0.178
11	120	0.45	0.126	30	1.14	0.145
12	120	0.43	0.117	30	1.15	0.148
13	120	0.45	0.130	30	1.11	0.144
14	120	0.50	0.158	30	1.15	0.166
15	120	0.51	0.130	30	1.14	0.183
16	120	0.49	0.155	30	1.15	0.183
17	120	0.48	0.170	30	1.19	0.187
18	120	0.49	0.140	30	1.13	0.200
19	120	0.45	0.119	30	1.11	0.174
20	120	0.41	0.133			
21	120	0.42	0.120			
22	120	0.44	0.131			
23	120	0.54	0.139			
24	120	0.56	0.158			
25	120	0.43	0.176			
26	120	0.50	0.153			
27	120	0.46	0.143			
28	120	0.48	0.135			
29	120	0.47	0.120			
30	120	0.47	0.134			

Notes. The seeing values are measured by the DIMM seeing monitor in the V band and the FWHM value corresponds to the one measured in the extracted PSF, used to fit the positions of the stars. In the case of the NGC 6388 data, the first five frames are taken using only ground-layer correction and frames 6–30 are in full MCAO mode. In the case of the 47 Tuc data all frames are taken using ground-layer correction.

cluster (RA(J2000)=00:24:05.6, DEC(J2000)=-72:04:49.4) was observed with the narrow-band Bry filter (central wavelength = $2.166 \mu\text{m}$) and 4 guide stars between $V = 11.9 \text{ mag}$ and $V = 12.5 \text{ mag}$, positioned around the field with one guide star in the south-eastern corner of the field (Fig. 1, right side). We have analyzed 19 frames with DIT = 2 sec and NDIT = 15, corresponding to a total exposure time of 30 seconds per frame.

2.3. Data reduction

Each science frame was flatfield corrected by the flatfield image obtained from sky flats taken at the beginning of the night

¹ HST F606W photometry data

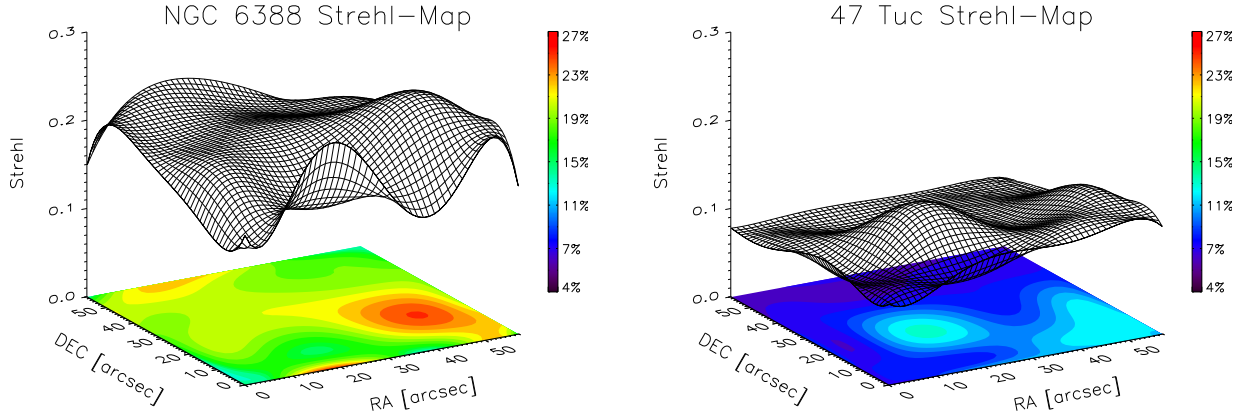


Fig. 2. Example Strehl maps for one of the NGC 6388 (left) and 47 Tuc (right) data set, respectively.

and badpixel corrected with a badpixel mask obtained from the same flat-field images (Moretti et al. 2009). Sky subtraction was done by median combining all sky and science frames to one single sky frame. This frame was then normalized to the median counts of the science frames before subtraction. In the case of 47 Tuc no flat-field images were taken in Br_γ (central wavelength = $2.166 \mu\text{m}$) in that night. Consequently, we used the same flat-field image for correction as for the NGC 6388 data observed in K_s (central wavelength = $2.12 \mu\text{m}$). In the case of the NGC 6388 data, jittering was used during the observations and we cut all images to the common FoV after the data reduction. This left a slightly smaller field of the size of $1517 \text{ px} \times 1623 \text{ px}$ ($42.5'' \times 45.4''$). Only stars which were detected in all frames were used in the following astrometric analysis.

3. Strehl Maps

As a check of the AO performance we generated Strehl-maps by calculating the Strehl-ratio for each detected star. After interpolating values for areas where no stars were found, a smooth surface was fitted to the data, leading to a two dimensional Strehl-map for each frame. In Fig. 2 one example of these maps is shown for each data set.

The Strehl is fairly even over the field of view, mean values are between 10% - 23% in the full MCAO case and between 9% - 14% in the GLAO case, with a small drop-off to the edges of the field. This shows how uniformly the layer oriented MCAO approach corrects wavefront distortions. The drop-off to the edges of the FoV can partly be explained by the MCAO and the atmospheric tomography approach. The light coming from the different directions of the guide stars is optically co-added and a correction is computed based on this light distribution. But the footprints of the columns above the telescope in the direction of the guide stars overlap more in the middle of the field than at the edges in the higher layer. If the control software is not optimized to correct over the whole FoV very evenly, the middle of the field will be corrected better. As the data analyzed here is the first data of MCAO in layer oriented mode, we are not surprised to see such an effect. A performance evaluation of these data can be found in Arcidiacono et al. (2008). In the case of 47 Tuc the Strehl is smaller than in the case of the NGC 6388 data. GLAO works as a seeing reduction and Strehl ratios of a few percent are expected. The performance of the ground layer correction was therefore even better than expected, which was most probably due to the fact that during the ground layer obser-

vations the turbulence was particularly concentrated in this layer. MCAO should retrieve larger and more uniform Strehl ratios of the order of 20%-30% and diffraction limited FWHM values. Therefore the MCAO corrections did not yet fully reach the expectations. Nevertheless, an even Strehl ratio of $\sim 10\%$ or more over a $1' \times 1'$ FoV is already an enhancement compared to the seeing limited and the single guide star case, where the Strehl is varying with the separation to the guide star Roddier (1999); Cresci et al. (2005).

4. Astrometric measurements

4.1. Position measurements

To measure the positions of the stars in the single images of both clusters we used the program *StarFinder* (Diolaiti et al. 2000b,a), which is an IDL based code for PSF fitting astrometry and photometry in AO images of stellar fields. The following description accounts for both data sets.

We extracted the Point Spread Functions (PSF) for fitting the stars directly from the images, by using in each frame the same 30 stars to create the PSF by averaging these stars after deleting close secondary sources. The selected stars are evenly distributed over the FoV and are composed of brighter and fainter ones, with magnitude ranges of $K = 11 - 15.3$ in the NGC 6388 data and $K = 6.3 - 12.2$ in the 47 Tuc data. We assumed here, that the PSF does not vary strongly across the FoV. Analysis and tests we performed on the distributions of the eccentricity and orientation of the PSFs in the full FoV did not show a prominent variation over the field. The eccentricities and the orientations of the PSFs were analyzed by fitting a 2-dimensional Moffat function to the individual PSFs with the IDL based non-linear least square fitting package *mpfit2dpeak*, provided by Craig Markwardt (Markwardt 2009). Results from e.g. Schödel (2010) and Fritz et al. (2010) show that the PSF variation due to anisoplanatism can add an error to the position measurement of up to 0.1 pixel. These numbers were calculated for a classical AO correction with the S27 camera of the VLT/NACO instrument which has a similar image scale as the MAD detector (27.15 mas/px (NACO) vs. 28 mas/px (MAD)), but uses only one AO reference star, located somewhere in the FoV. The data analyzed here are the first ones obtained with multi-conjugated AO correction in the layer-oriented approach. These two circumstances lead to a more uniform PSF over the full FoV, as can also be seen in the even Strehl distribution (see

§ 3). Another confirmation that this assumption is acceptable can be seen in the case of the 47 Tuc data set. One of the used guide stars lies within the FoV (south-eastern corner, see Fig. 1 right side). Inspection of the eccentricity and orientation of the PSFs shows that the guide star does not differ in shape and orientation from the other stars. A behaviour, such as the change of the PSF dependent on the separation of the stars from the guide star, as in the classic AO correction, cannot be seen. After deleting false detections we matched the starlists to find the stars common to all frames. This left ~ 130 stars for the NGC 6388 field and ~ 280 stars for the 47 Tuc field.

4.2. Distortion correction

To investigate the stability of the MCAO and GLAO performance in terms of astrometric precision over time, we first corrected for distortions of the field. During the observations, malfunctioning of the de-rotator occurred due to a software problem, leading to a bigger rotational error in several frames. If the AO correction is very stable over time, the relative positions of the stars should be the same after correcting for effects such as the de-rotator problem (Arcidiacono et al. 2010). A misposition of the reference star on the tip of the pyramid-WFS exceeding a few λ/D (where λ is the wavelength and D the telescope diameter) with respect to the theoretical (unrotated) positions, affects also the closed loop performance, generating a correction under-performance. We set up a master-coordinate-frame to which the single frame coordinates are later mapped. In order to create this coordinate frame, we used the best frame, chosen according to the highest mean Strehl ratio in the images, as a first reference frame and mapped all the stellar positions from each individual frame onto this reference frame by calculating the shift and scale in x - and y -direction and the rotation between these frames. The MIDAS² data reduction software and simple affine transformations were used for the transformations. We did not apply any interpolation directly to the images, but instead worked with the measured coordinates. After correcting for the derived rotation for each frame, as well as for the shift and scale in x and y of each stellar position, a master-coordinate-frame was created by averaging the position of each star over all frames. The so derived coordinate frame with averaged positions was then used as the master-coordinate-frame for the coming analysis.

In the following, regarding the necessary distortion correction of each single frame, we analyzed the data using two approaches. In a first attempt we corrected only basic distortions, including shift, scale and rotation. To furthermore explore the full capacity of astrometry with MCAO, we performed a second distortion correction which included higher order terms.

4.2.1. Basic distortion correction

Once we created the reference frame for each data set, all coordinates from each single frame were then mapped to this master-frame, leading to a better calculation of the transformation parameters for the individual frames. One might think that one can achieve even better transformations between the frames by applying this method iteratively, creating once more a master-coordinate-frame. If the distortions in the images, those left over from the AO or systematic ones, were homogeneous

over the FoV, the transformations should not change or enhance the positions of the master-coordinate-frame a lot. But if the distortions are not homogeneous, but depend, for example, on the camera position in the FoV, one would introduce warpings in the master-coordinate-frame which one cannot map with a simple combination of shifting, scaling and rotation anymore. We therefore stopped after one iteration.

We then calculated the residual separations between the positions of the stars in the master-coordinate-frame to the positions in the individual frames, calculated with the obtained transformation parameters and analyzed them as a measure of astrometric precision.

4.2.2. Separation Measurements

To evaluate the astrometric precision and stability of MCAO data, we measured the relative separations between various pairs of stars all over the FoV before and after applying the calculated distortion corrections. For this we derived a time sequence of the separation over all frames. If only a steady distortion were present in the single frames, then the separations should be stable over time or only scatter within a certain range given by the accuracy of the determination of the position of the stars, which is 0.33 mas for the faintest star used in this analysis. If differential distortions between the single frames are present, but these distortions are random, the scatter of the separations is expected to increase, depending on the strength/amplitude of the differential distortions. A not perfectly corrected defocus, for example, would change the absolute separation between two stars, but, to first order, not the relative one measured in the individual frames, if this defocus is stable over time. An uncorrected rotation between the frames would change the separation of two stars in the x and y direction, but not their separation, $r = \sqrt{\Delta x^2 + \Delta y^2}$.

Performing this test for several star pairs with short and large separations and with different position angles between the stars before any distortion correction, showed in the case of the NGC 6388 data a recurring pattern in the separation in x, y, r , which is not observable in the 47 Tuc data. Fig. 4 shows the separation in x, y and r over the frame number for five representative pairs of stars in the NGC 6388 data. Looking at the pattern, which repeats after five frames for the first 10 frames and after 10 frames for the following frames (where always two images were taken at the same jitter position before moving to the next position), one finds that this change in separation seems to be correlated with the jitter movement during the observations which also has a five points pattern with an additional change of the center position. In the case of the MAD instrument the camera itself is moved in the focal plane to execute the jitter pattern. This can lead to vignetting effects for larger jitter offsets and distortions seem to be introduced, dependent on the position of the camera in the field of view. It is unlikely that this pattern is due to the problems with the de-rotator, because of the uniform repetition of the pattern. Also this pattern is not seen in the 47 Tuc data, which was obtained without jitter movements, but experienced the same de-rotator problems.

We performed the same measurements of the same star pairs after applying the calculated distortion correction for shift, scale and rotation. The strong pattern is gone, leaving a more random variation of the separation. Also the calculated standard

² <http://www.eso.org/sci/data-processing/software/esomidas/>

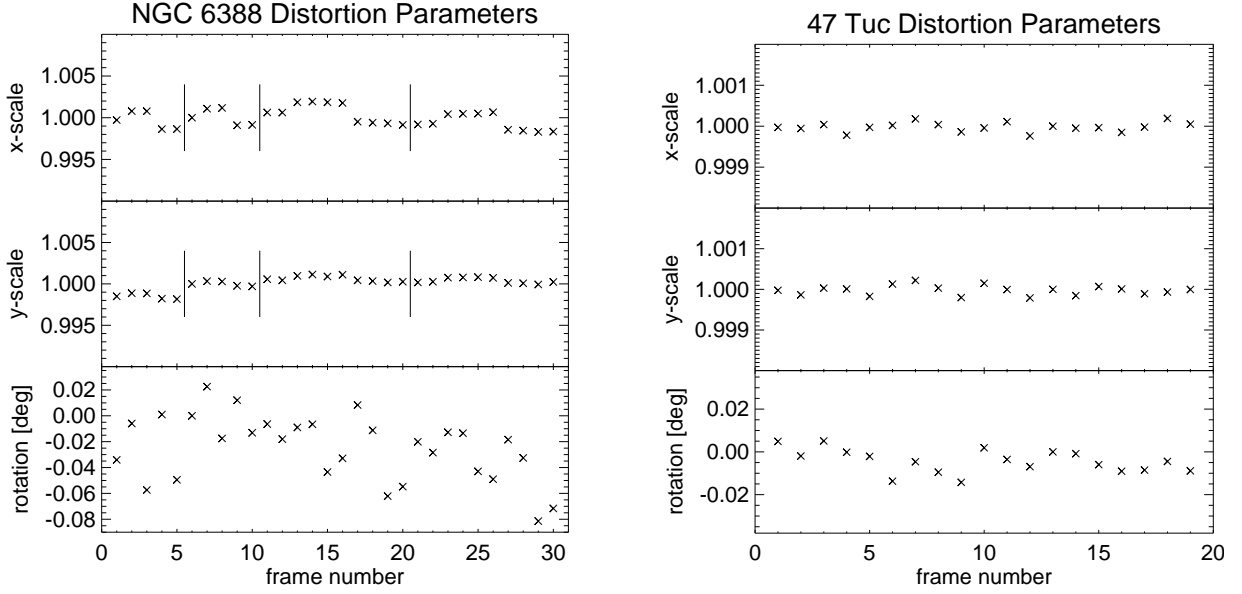


Fig. 3. Applied distortion parameters for the basic distortion correction over frame number for the NGC 6388 (left) and 47 Tuc data (right). The panels show from top to bottom the calculated distortion parameters for x scale, y scale and rotation for each frame. While the rotation parameter is random, the scale parameter of the NGC 6388 data shows a pattern which is not visible in the 47 Tuc data. The vertical lines indicate after which frame the jitter movement of five positions (five or ten frames) was repeated and highlight the introduced pattern.

deviation is much smaller, ranging from a factor of ~ 3 up to a factor of ~ 19 times smaller. Comparing the single standard deviations shows a smaller scatter among their values than before the distortion correction. All this leads to the conclusion, that the calculated and applied distortions remove a large amount of the separation scatter, but not all of it. The remaining scatter of the separations between the stars in the single frames still ranges from $\sim 1.2 - 2.8$ mas, well above the scatter expected from photon statistics, pointing to uncorrected higher-order distortions.

4.2.3. Basic distortion parameters

The calculated distortion parameters from the basic distortion correction for x -scale, y -scale and rotation over the frame number, which can be seen as a time-series, are plotted in Fig. 3 for both data sets. Whereas the parameter for the rotation correction looks random, but with a fairly large scatter indicating the de-rotation problem, the correction parameters for the scale in x and y show a pattern in the case of the NGC 6388 data set (left). This pattern repeats after five (10) frames, as does the pattern for the separation measurement. As these are the applied correction parameters, they nicely show the existence of the pattern and our ability to correct for this induced scale variation due to the jitter movement. In the 47 Tuc data there is also some scatter, which can be expected, but no repeating pattern can be seen. Additionally, the values are smaller in the case of these ground layer corrected data which were obtained without jitter (note the different scaling of the two plots).

4.3. Higher order distortion correction

We additionally performed a comparison of the individual frame stellar positions with the reference positions by applying a poly-

nomial fit including also higher order transformation terms. To derive the transformation coefficients, we used the IDL routine *POLYWARP*, which is able to fit a polynomial function of several orders, using a least squares algorithm (see e.g. also Schödel et al. 2009). The polynomial functions used are:

$$X_i = \sum_{i,j} K_{x_{i,j}} X_0^j Y_0^i \quad (1)$$

$$Y_i = \sum_{i,j} K_{y_{i,j}} X_0^j Y_0^i \quad (2)$$

where X_i, Y_i are the reference stellar positions and X_0, Y_0 the stellar positions in the individual frames. $K_{x_{i,j}}, K_{y_{i,j}}$ are the coefficients to be calculated. After performing the fit with orders from $i, j \leq 1 - 10$, we decided to perform the final transformation with an order of $i, j = 4$.

A fit of order four gives an enhancement of 6-10% (NGC 6388) and 14-19% (47 Tuc) of the remaining mean residuals compared to the fit of order 3. Fitting even higher orders is not necessary, as no significant enhancement of the residuals can be seen. After transformation of the stellar positions in the individual frames to the common reference frame, the residual separations were calculated as in the case of the simpler transformations, see § 4.2.3.

5. Results

The basic distortion corrections are sufficient for high accuracy photometry (Moretti et al. 2009), but to achieve the highest astrometric precision, a distortion correction including higher orders is necessary. We therefore performed a higher order distortion correction and show the compelling results in the following paragraph.

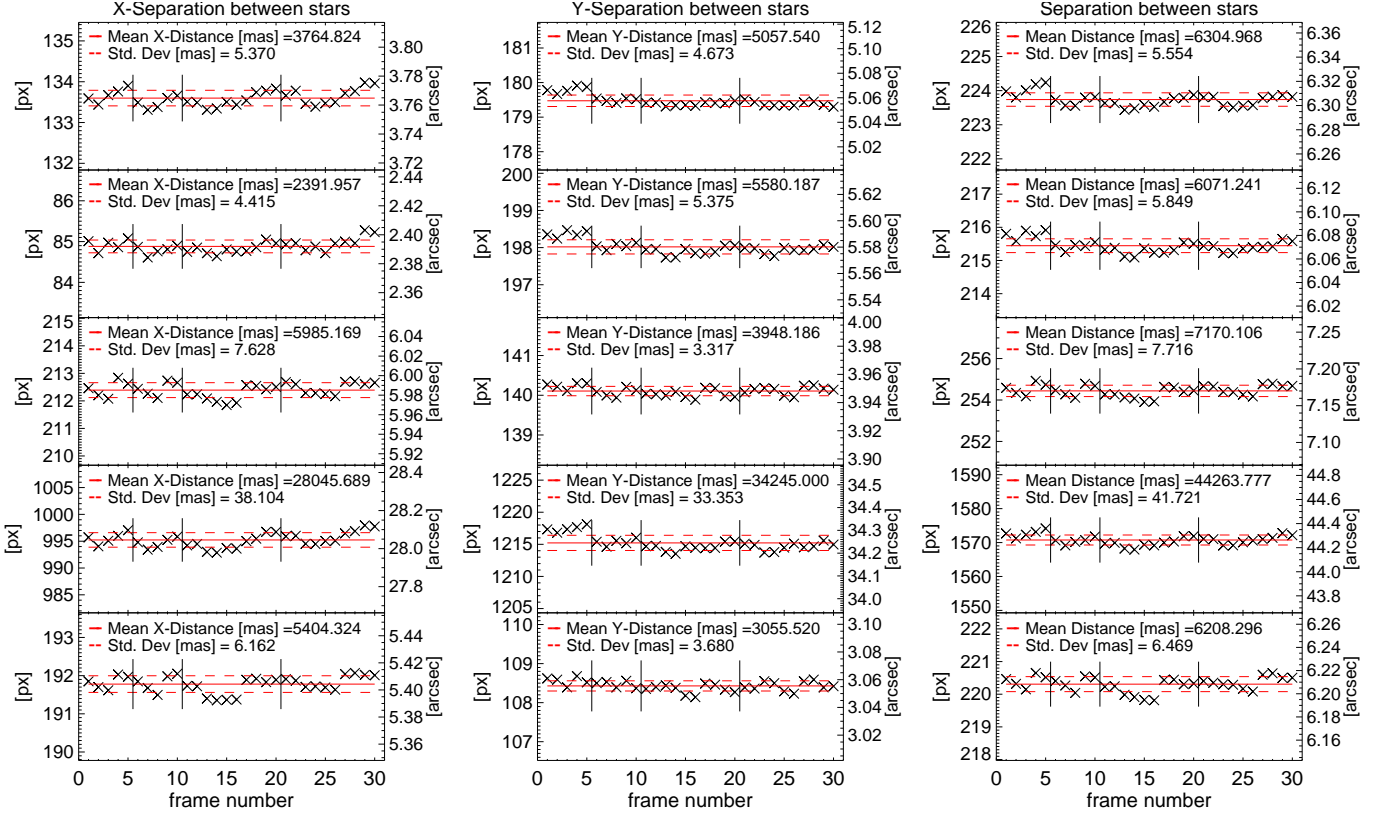


Fig. 4. Separation between pairs of stars in the NGC 6388 data set plotted against frame number before any distortion correction. The left panel shows the separation in x-direction, the middle panel in y-direction and the right panel the full separation $r = \sqrt{\Delta x^2 + \Delta y^2}$. The left y-axes are given in *pixel* while the right ones give the measured distances in seconds of arc. The small straight lines mark the frames after which a new five points sequence of jitter movements was started. The x-axes can also be seen as a time sequence as the individual frames were obtained subsequently, the first ten with an exposure time of 240 s and the last 20 with an exposure time of 120 s.

5.1. Residual Mapping

After calculating the residuals for each frame with respect to the master-coordinate-frame, we analyzed the distribution of these residuals over the field of view.

We analyzed contour plots of the residuals by fitting a minimum curvature surface to the data of each frame to look at the spatial distribution of the residuals after the distortion correction. The main goal of this test was to check for any strong spatial variation of the residuals over the FoV. No strong spatial variation can be seen, such as for example a strong gradient in one direction. Additionally we analyzed arrow diagrams showing not only the strength, but also the direction of the residuals for each star used to calculate the transformation. We found the orientation of the arrows to be random.

Finally, we calculated the mean residuals over the full FoV for both data sets separately for the x , y and r ($r = \sqrt{\Delta x^2 + \Delta y^2}$) direction for each frame. The mean values are very close to zero ($\sim 10^{-5} - 10^{-6}$ pixel), supporting the results from the arrow plots of random orientation, but the mean of the *absolute* values of the residuals provides a better indicator for the variability present in the data. In Fig. 5 the mean of the absolute values of the residuals over the full FoV in the x and y directions and in the separation r are plotted over the diameter of 50% ensquared energy of the corresponding extracted PSF of each frame and

each data set. In the case of an image where the flux is given as flux per pixel, like any detector image, the ensquared energy is defined as the flux of a PSF within a certain quadratic box with the size of $n \times n$ pixel divided by the total flux. The smaller the side length (=diameter) of this box, containing 50% of the total energy, the better the AO correction, moving flux from the wings into the core of the PSF. No correlation of the size of the residuals with the ensquared energy and therefore the performance of the AO system can be seen in the 47 Tuc data set, but there is a small correlation in the NGC 6388 data. What is visible, is that the absolute values of the residuals and their scatter are larger in the case of the NGC 6388 data set compared to the 47 Tuc data set, even though the initial observing conditions were better and the measured FWHM values and diameters of 50% ensquared energy are smaller. Compared to a only basic correction of the image distortions (crosses \times), the residuals after a higher order correction (diamonds \diamond) are noticeable smaller and do not scatter as much as in the case of the basic distortion correction, showing the superiority of the higher order correction.

The values after the higher order correction give a first impression of how precise the astrometry is in these MAD data. The mean absolute residuals are between 0.020 px and 0.068 px (0.55 - 1.90 mas) in the x -direction and between 0.028 px and 0.060 px (0.78 - 1.68 mas) in the y -direction in the MCAO corrected NGC 6388 data set. In the case for the ground layer

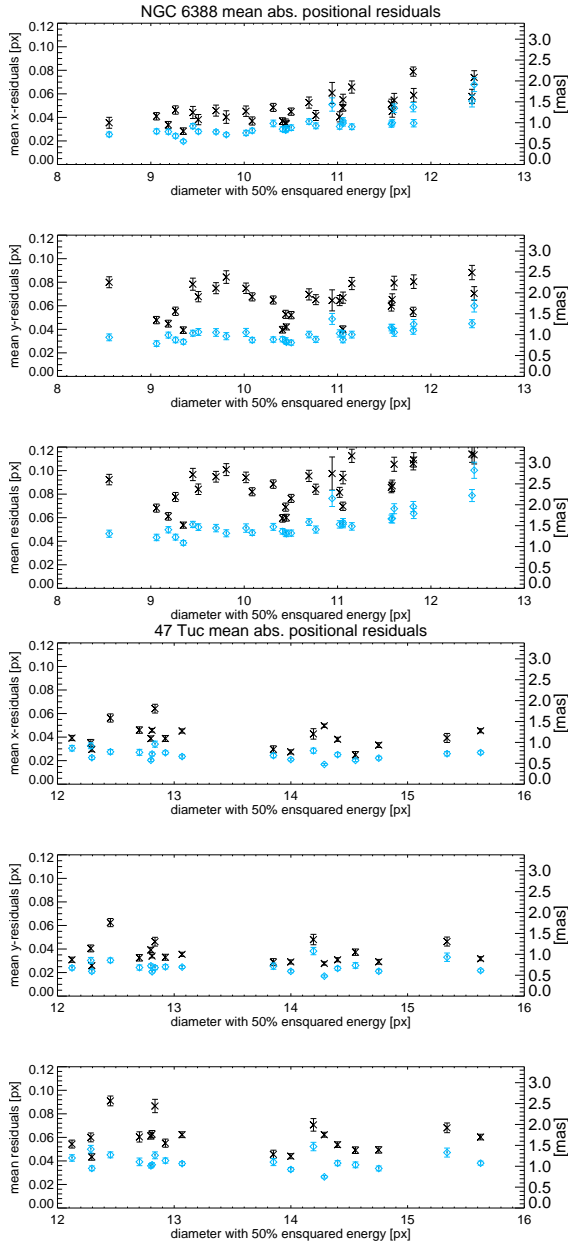


Fig. 5. Mean of the absolute values of the positional residuals over the diameter of 50% ensquared energy. In the upper panels for the NGC 6388 data set and in the lower panels for the 47 Tuc data set. The plot shows from top to bottom the mean of the absolute values of the residuals to the masterframe in the x - and y -direction and the separation $r = \sqrt{x^2 + y^2}$ after a 4th order polynomial correction (diamonds \diamond) and after the correction of x and y -shift, x and y -scale and rotation (crosses \times). The overplotted error bars correspond to the error of the mean value σ/\sqrt{n} , with n equal to the number of stars used to calculate the mean value and σ being the standard deviation. The left y -axis shows the residuals in units of pixel and the right one in units of mas.

corrected 47 Tuc data set, the absolute values of the residuals are between 0.017 - 0.034 px (0.47 - 0.95 mas) and 0.017 - 0.038 px (0.47 - 1.07 mas) in the x and y direction, respectively. With photon statistics alone, the positions should have a smaller range of variation. Taking the positional accuracy calculated from photon statistics for the faintest stars used in this set, the

residuals should be within 0.012 px (0.33 mas) and 0.011 px (0.32 mas) in x and y direction, respectively, in the NGC 6388 case and 0.005 px (0.14 mas) for both, x and y , in the 47 Tuc case. The accuracies $\Delta x, \Delta y$ from photon statistics were thereby calculated by: $\Delta x/y = \frac{FWHM_{x/y}}{\sqrt{n}}$, where $FWHM_{x/y}$ is the Full Width at Half Maximum of the fitted PSF in x and y , respectively and n the number of photons of the fitted star.

The basic distortion correction, where we only accounted for shift, scale and rotation, shows a residual positional scatter that cannot be explained by simple statistical uncertainties. It rather shows that even after a basic distortion correction, there is remaining positional scatter, which seems to have its origin in higher order distortions present in the images, as it seems largely independent from the size of the PSF.

The residuals after the higher order corrections show a significant enhancement in the precision, even though the values are still larger than the ones taking only photon statistics into account. But one has to remember that the latter values only show the lower limit of the possibly reachable positional accuracy. In reality the uncertainties will likely be larger, possibly due to locally by the AO correction induced distortions, which cannot be well described by polynomials and/or errors from the PSF estimation and fit.

Additionally, the residuals and scatter are larger in the case where the camera was jittering to scan a bigger field of view. This jitter movement introduced distortions, which were already visible in the separation measurements and in the distortion correction parameters calculated for scale and rotation, see § 4.2.3. But also the AO correction can introduce distortions, as it dynamically adapts to atmospheric turbulence changes. With only these two data sets available in the LO correction mode, which are suitable for this analysis, it is not possible at this time to separate the different error sources. Although in the case of the 47 Tuc data where no jitter movement was performed, the residuals can be interpreted as effects of correcting only the ground layer and the AO correction itself.

5.2. Mean Positions

As a last step we calculated the mean position for each star over all corrected frames and its standard deviation as a measure of astrometric precision. In Fig. 6 the achieved astrometric precision is plotted over the K magnitude for each star in the final lists of both data sets (blue \times). The given magnitude represents the estimated 2MASS (Skrutskie et al. 2006) K magnitude of the stars, which suffices to see the principal relation between precision and intensity. For completeness the total counts are indicated at the upper x -axis of the plots. These values show that we compare stars within the same detected flux range, even though the magnitude ranges differ. This is due to the fact that in the case of the observations of the cluster 47 Tuc the Br_γ narrow-band filter was used instead of the broader K_s -filter and the exposure times were reduced compared to the observations of NGC 6388.

As one can see in the plots in Fig. 6 for the NGC 6388 data set (left panels), the fainter stars have less precision in their position than the brighter ones. The mean positional precision of the stars between 14 and 18 mag after the full distortion correction is 0.041 pixel corresponding to 1.143 mas in the x -direction and 0.046 px (1.278 mas) in the y -direction, where x is parallel to the right ascension and y to the declination axes. The median

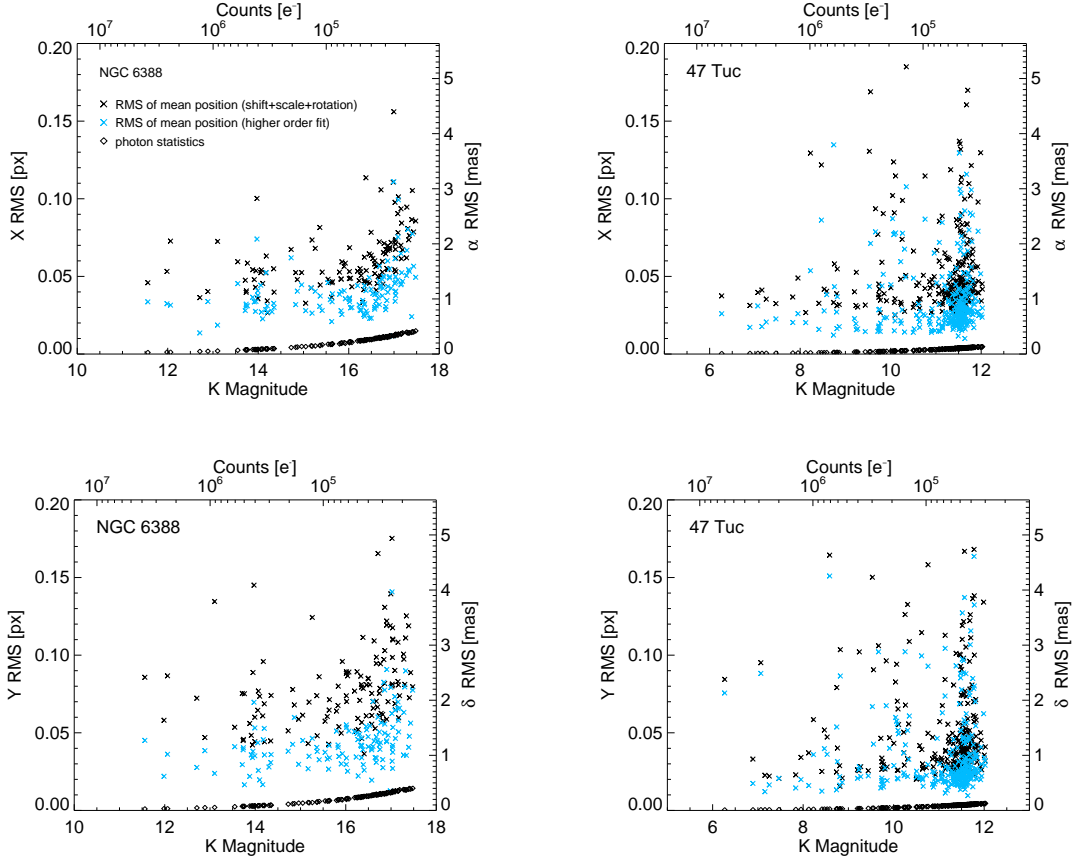


Fig. 6. MAD positional RMS (\times), calculated over all frames as function of the corresponding 2MASS K -magnitude for both, the higher order correction (blue) and the basic distortion correction (black). The left panels show the data of the NGC 6388 cluster which was observed with the full MCAO mode for the x - and y -direction and the right panels show the data of the 47 Tuc cluster, observed with ground layer correction. For comparison the position precision calculated from photon statistics as the median of all frames is also shown (\diamond).

value of the precision in this magnitude range is slightly smaller, x : 0.039 px (1.084 mas), y : 0.042 px (1.179 mas). This is the achievable astrometric precision with the available MAD data in full MCAO mode. Theoretically, as stated above in § 5.1, the faintest stars in this regime should have a precision of about 0.015 px (0.420 mas) assuming only photon statistics and then the mean positional precision in the same magnitude range of $K = 14 - 18$ mag is 0.009 px (0.252 mas) in the x - and y -direction. The mean precision from photon statistics was thereby calculated by taking the median of the positional precisions of each star in all individual frames. These estimates for each star are also shown in Fig. 6, plotted as diamonds. The measured precision of the mean position is a factor of 4.6 (x -direction) and 5.1 (y -direction) worse than the one estimated from photon statistics. This is a quite large discrepancy, although one has to take more than simple photon statistics into account for calculating a correct error budget, as for example the error from the PSF estimation which was used to fit the stellar positions and to calculate the uncertainty estimates.

In the GLAO data set of 47 Tuc the astrometric precision for stars with corresponding 2MASS magnitudes between 9 and 12 mag is 0.034 pixel (0.960 mas) and 0.035 pixel (0.972 mas) in the x - and y directions, respectively. The median value is 0.027 px (0.750 mas) in x and 0.025 px (0.699 mas) in y .

Although the fainter stars seem to have slightly larger uncertainties, this correlation is less distinctive than in the MCAO case (NGC 6388). For comparison, the results from the basic distortion correction are also plotted in Fig. 6 as black crosses.

In Tab. 2 the above described results for the higher order correction are summarized.

Comparing the results for the ground layer correction with those of the MCAO correction shows a higher precision in the GLAO data. One would expect it the other way round as the initial observing conditions and the average Strehl are better in the MCAO data plus the MCAO correction is expected to correct the wavefront distortions more accurately. Also the FWHM and the diameter of 50% ensquared energy are smaller in the MCAO data. One of the main differences in the two data sets is the jitter movement. As already shown, this movement introduces distortions.

In a first attempt we corrected only for shift, scale and rotation, but the afterwards achieved precision is worse than expected, indicating distortions of higher order. Correcting both data sets also for higher order distortions leads to a higher precision on both, the NGC 6388 and the 47 Tuc data, but still a better cor-

Table 2. Summary of the expected and achieved astrometric precisions after a distortion correction including higher orders.

unit	NGC 6388, $K = 14-18$					47 Tuc, $K = 9-12$				
	mean		median		Photon statistics	mean		median		Photon statistics
	x	y	x	y		x	y	x	y	
px:	± 0.041	± 0.046	± 0.039	± 0.042	± 0.009	± 0.034	± 0.035	± 0.027	± 0.025	± 0.005
mas:	± 1.143	± 1.278	± 1.084	± 1.179	± 0.252	± 0.960	± 0.972	± 0.750	± 0.699	± 0.084

rection in the pure ground-layer correction can be seen (which is also observed without jitter movements).

6. Conclusions

We have analyzed the first multi conjugated adaptive optics data available in the layer oriented approach with respect to astrometric performance. The data were taken with the MCAO demonstrator MAD at the VLT. Two sets of data of globular clusters, observed in two different approaches were analyzed: the globular cluster 47 Tucanae with ground layer correction only and the globular cluster NGC 6388 in full two-layer MCAO correction.

As a performance measure we calculated Strehl maps for each frame. The Strehl is fairly uniform over the FoV with a small degradation toward the edges of the FoV and average values between 11% and 23% in the MCAO data and between 9% and 14% in the GLAO data. The lower Strehl in the 47 Tuc data set may partly be explained by the fact that only the distortions due to the ground layer were corrected, but also the initial atmospheric conditions were worse.

After extensive PSF tests we analyzed the data with the *StarFinder* code. We created a master frame with positions of isolated stars in the field and calculated in a first attempt distortion parameters for shift and scale in x - and y -direction and a rotation for each frame to this master frame. Separation measurements between stars before and after the distortion correction showed that these corrections are indeed reducing the scatter in the separations measured over all frames (§ 4.2.2). But it also shows a residual scatter, which is probably due to higher order distortions. A pattern visible in the separation measurements (Fig. 4) as well as in the applied distortion parameters (Fig. 3) is thought to be due to the jitter movement of the camera during the observations. This movement introduced additional distortions which could only be corrected partly, with this distortion correction. To exploit the full capacity of astrometry with MCAO we performed a 4th order polynomial distortion correction, including also higher order terms.

The mean precision of the positions of the stars, calculated by the scatter of the mean position of the stars over all frames, is 0.041 pixel (1.143 mas) and 0.046 pixel (1.278 mas), for the x - and y -direction, respectively, in the corresponding 2MASS K magnitude range from 14 to 18 mag in the NGC 6388 data set (MCAO). In the 47 Tuc data set (GLAO) the mean precision is 0.034 pixel (0.9602 mas) and 0.035 pixel (0.972 mas) for comparable K magnitudes between 9 and 12.

These results show impressively the capacity of high precision astrometry over a large field of view observed with MCAO.

An astrometric analysis of the core of 47 Tuc was also performed by McLaughlin et al. (2006), who used several epochs of data from the Hubble Space Telescope (HST). They derived positional precisions in the single epoch data, for stars in the same area as the here analyzed FoV, taken with the High Resolution Camera (HRC) of the Advanced Camera for Surveys (ACS) for most stars in the range of 0.01-0.05 pixel. With a plate-scale of 0.027 arcsec/pixel this corresponds to 0.27-1.35 mas. The errors were calculated in the same way as in this work, taking the standard deviation of the positions in all frames as uncertainties. Detailed distortion corrections were computed for ACS by Anderson (2002), which were applied to the data in the work of McLaughlin et al.. This shows that the precision derived with MAD is already comparable to HST/ACS astrometry and with a good distortion characterization, future instruments could yield even higher astrometric precision.

Although the Strehl-ratio is smaller and the FWHM is larger in the GLAO data of the cluster 47 Tuc, the achieved astrometric precision is higher. Also the observing conditions were worse during the GLAO observations compared to the MCAO observations with a mean seeing of 1.13'' and 0.46'', respectively. All this leads to the conclusion that the degradation of the astrometric precision in the MCAO data set is mainly due to the jitter movement during the observations, which introduced additional distortions. But also the more complex correction of two layers could have introduced distortions, which we could not correct for. To fully characterize the remaining distortions, one would need to analyse more data, taken under various seeing conditions and observation configurations. As MAD will not be offered again, a fully satisfactory analysis is not possible at this point. Nevertheless one can interpret the remaining positional uncertainty in the GLAO corrected data, which was obtained without any jitter movement, as distortions remaining from the AO correction and not compensated turbulence.

All the results presented here are still given in detector coordinates, as we analyzed the data in matters of the adaptive optics correction and instrumentation stability over the time of the full length of the observation. Going to celestial coordinates would involve the correction for effects such as differential aberration and differential refraction to derive the true positions of the stars. As the observed FoV is large, these effects can reach several milliseconds of arc of displacement between stars at different points on the detector (Meyer et al. 2010, in preparation). These transformations introduce additional position uncertainties, degrading the astrometric precision further, but need to be performed when comparing data from different epochs, as for example in proper motion studies. The data analyzed here is single epoch data, therefore these corrections did not need to be performed to investigate the stability and possible accuracy of astrometric

measurements in MCAO data, as these are effects present in all ground-based imaging data and do not influence or are influenced by the AO performance.

To make a final comparison between ground-based MCAO and space-based astrometric precision, a multi-epoch study needs to be carried out. As MAD is not offered again, this is not possible at the current state and with the available data.

Acknowledgements. The data analyzed here are based on observations collected at the European Southern Observatory, Paranal, Chile, as part of the MAD Guaranteed Time Observations. We would like to thank the anonymous referee for the useful comments and suggestions to this paper.

References

- Anderson, J. 2002, in *The 2002 HST Calibration Workshop : Hubble after the Installation of the ACS and the NICMOS Cooling System*, ed. S. Arribas, A. Koekemoer, & B. Whitmore, 13–+
- Arcidiacono, C., Lombini, M., Diolaiti, E., Farinato, J., & Ragazzoni, R. 2006, in *Society of Photo-Optical Instrumentation Engineers (SPIE) Conference Series*, Vol. 6272, 627227
- Arcidiacono, C., Lombini, M., Moretti, A., et al. 2010, in *Society of Photo-Optical Instrumentation Engineers (SPIE) Conference Series*, Vol. 7736, Society of Photo-Optical Instrumentation Engineers (SPIE) Conference Series
- Arcidiacono, C., Lombini, M., Ragazzoni, R., et al. 2008, in *Society of Photo-Optical Instrumentation Engineers (SPIE) Conference Series*, Vol. 7015, Society of Photo-Optical Instrumentation Engineers (SPIE) Conference Series
- Bean, J. L., McArthur, B. E., Benedict, G. F., et al. 2007, *AJ*, 134, 749
- Beckers, J. 1988, in *Very Large Telescopes and their Instrumentation*, ESO Conference and Workshop Proceedings, p.693, Garching, March 21-24, 1988, edited by Marie-Helene Ulrich., 693
- Benedict, G. F., McArthur, B. E., Forveille, T., et al. 2002, *ApJ*, 581, L115
- Cresci, G., Davies, R. I., Baker, A. J., & Lehnert, M. D. 2005, *A&A*, 438, 757
- Diolaiti, E., Bendinelli, O., Bonaccini, D., et al. 2000a, 147, 335
- Diolaiti, E., Bendinelli, O., Bonaccini, D., et al. 2000b, in *Presented at the Society of Photo-Optical Instrumentation Engineers (SPIE) Conference*, Vol. 4007, Society of Photo-Optical Instrumentation Engineers (SPIE) Conference Series, ed. P. L. Wizinowich, 879–888
- Ellerbroek, B. L., van Loan, C., Pitsianis, N. P., & Plemmons, R. J. 1994, in *Society of Photo-Optical Instrumentation Engineers (SPIE) Conference Series*, Vol. 2201, Society of Photo-Optical Instrumentation Engineers (SPIE) Conference Series, ed. M. A. Ealey & F. Merkle, 935–948
- Farinato, J., Ragazzoni, R., Arcidiacono, C., et al. 2008, in *Society of Photo-Optical Instrumentation Engineers (SPIE) Conference Series*, Vol. 7015, Society of Photo-Optical Instrumentation Engineers (SPIE) Conference Series
- Fritz, T., Gillessen, S., Trippe, S., et al. 2010, *MNRAS*, 401, 1177
- Hubin, N., Marchetti, E., Fedrigo, E., et al. 2002, in *European Southern Observatory Astrophysics Symposia*, Vol. 58, European Southern Observatory Astrophysics Symposia, ed. E. Vernet, R. Ragazzoni, S. Esposito, & N. Hubin, 27–+
- King, I. R. & Anderson, J. 2001, in *Astronomical Society of the Pacific Conference Series*, Vol. 228, Dynamics of Star Clusters and the Milky Way, ed. S. Deiters, B. Fuchs, A. Just, R. Spurzem, & R. Wielen, 19–+
- Marchetti, E., Brast, R., Delabre, B., et al. 2007, *The Messenger*, 129, 8
- Marchetti, E., Hubin, N. N., Fedrigo, E., et al. 2003, in *Society of Photo-Optical Instrumentation Engineers (SPIE) Conference Series*, Vol. 4839, Society of Photo-Optical Instrumentation Engineers (SPIE) Conference Series, ed. P. L. Wizinowich & D. Bonaccini, 317–328
- Markwardt, C. B. 2009, in *Astronomical Society of the Pacific Conference Series*, Vol. 411, Astronomical Society of the Pacific Conference Series, ed. D. A. Bohlender, D. Durand, & P. Dowler, 251–+
- McLaughlin, D. E., Anderson, J., Meylan, G., et al. 2006, *ApJS*, 166, 249
- Meyer, E., Kürster, M., & Köhler, R. 2010, in preparation
- Moretti, A., Piotto, G., Arcidiacono, C., et al. 2009, *A&A*, 493, 539
- Ragazzoni, R. 1996, *J. Modern Opt.*, **43**, 289
- Ragazzoni, R., Farinato, J., & Marchetti, E. 2000a, in *Presented at the Society of Photo-Optical Instrumentation Engineers (SPIE) Conference*, Vol. 4007, Society of Photo-Optical Instrumentation Engineers (SPIE) Conference Series, ed. P. L. Wizinowich, 1076–1087
- Ragazzoni, R., Marchetti, E., & Valente, G. 2000b, *Nature*, 403, 54
- Rigaut, F. 2002, in *Beyond conventional adaptive optics : a conference devoted to the development of adaptive optics for extremely large telescopes*. Proceedings of the Topical Meeting held May 7-10, 2001, Venice, Italy. Edited by E. Vernet, R. Ragazzoni, S. Esposito, and N. Hubin. Garching, Germany: European Southern Observatory, 2002 ESO Conference and Workshop Proceedings, Vol. 58, ISBN 3923524617, p.11
- Rochau, B., Brandner, W., Stolte, A., et al. 2010, *ApJ*, 716
- Roddier, F. 1999, *Adaptive Optics in Astronomy* (Cambridge University Press)
- Schödel, R. 2010, *A&A*, 509, A58+
- Schödel, R., Merritt, D., & Eckart, A. 2009, *A&A*, 502, 91
- Skrutskie, M. F., Cutri, R. M., Stiening, R., et al. 2006, *AJ*, 131, 1163
- Tallon, M. & Foy, R. 1990, *A&A*, 235, 549
- Trippe, S., Gillessen, S., Gerhard, O. E., et al. 2008, *A&A*, 492, 419
- Yan, H., Wu, H., Li, S., & Chen, S. 2005, in *Society of Photo-Optical Instrumentation Engineers (SPIE) Conference Series*, Vol. 5903, Society of Photo-Optical Instrumentation Engineers (SPIE) Conference Series, ed. R. K. Tyson & M. Lloyd-Hart, 260–271